Ghana Journal of Geography

journal homepage: https://www.ajol.info/index.php/gjg/ https://journals.ug.edu.gh/index.php/gjg/

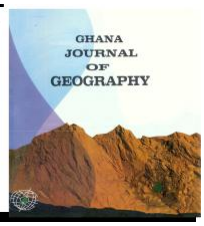

Non-Linear Responses to Land Use Change: Exploring Morphological Thresholds and Chaotic Signatures in the Ankobra River.

Julia Quaicoe [1] & Suleman Dauda [1*]

[1]Department of Geography and Regional Planning, Faculty of Social Sciences, University of Cape Coast, Cape Coast, Ghana

http://dx.doi.org/10.4314/gjg.v17i3.3

article info

Article history:
Received 21st September 2025
Accepted 23rd December 2025
Published 31st December 2025

Keywords:
River Morphology Predictability,
River Channel Evolution,
Chaos,
Ankobra River,
Ghana.

abstract

River systems often display complex and seemingly random behaviours and patterns. This complexity may be attributable to the non-linear dynamics intrinsic to these systems, making them suitable for analysis through the lens of chaos theory. While natural processes contribute to chaotic behaviour, human land-use and land-cover changes significantly alter river systems by modifying sediment loads, flow regimes, and riparian vegetation. In this study, we examine how land-use and land-cover changes can act as perturbations, triggering or amplifying chaotic dynamics in river systems, using the Ankobra River basin as a case study. The research utilizes satellite imagery, remote sensing (RS), and Geographic Information Systems (GIS) techniques for spatiotemporal quantification of river channel form and LULC changes over three (3) decades (1991-2024). Specifically, Landsat images were processed and analysed using 5.6 ENVI and ArcGIS Pro. Findings reveal a significant and consistent increase in built-up areas over the different periods in the various sections of the river, coupled with a notable decrease in dense and sparse vegetation observed over much of the study period. The study concludes that the behaviour of river systems is on a continuous trajectory where future dynamics is dependent critically on present actions, past events, and conditions that exists in both upstream and downstream reaches.

Introduction

River channels are fundamental components of the fluvial landscape. They are often described as self-formed gutters, where dimensions, patterns, gradients, and bed materials adjust dynamically through erosion and deposition (Lane & Richards, 1997; Church & Ferguson, 2015; Rego-Costa et al., 2017; Cunico et al., 2024). River channel patterns and morphologies are complex and highly dynamic, constantly shaped by the interplay of various physical and, increasingly, biological processes (Church & Ferguson, 2015). Despite the significant advancements in understanding the processes that drive river channel change, the inherent complexity and the multitude of factors acting across different spatial and temporal scales mean that predicting the precise spatial and temporal evolution of river patterns, such as channel width and sinuosity, especially in the long term, remains challenging (Cunico et al., 2024).

Similarly, river predictability is a complex concept that refers to the ability to foresee and forecast the future behaviour and changes within river systems (Rego-Costa et al., 2017; Cunico et al., 2024). This can be influenced by both internal river processes, including bifurcation and confluences, as well as riverbed evolution and sediment transport (Cunico et al., 2024; Durante et al., 2025; Hasan et al., 2025), and external influences such as Land Use Land Cover Changes (LULCC) (Kim et al., 2011). According to Hasan et al. (2025), LULC changes refer to alterations in the physical cover and human use of land, which significantly influence river systems by impacting their hydrology and morphology through altered sediment dynamics, streamflow variability, and alterations in runoff. These can generate non-linear interactions between flow, sediment, and vegetation leading to deterministic chaos, where even small initial changes can lead to vastly different outcomes over time as analogous to Lorenz's "Butterfly Effect," where a tiny air movement (like a butterfly flapping its wings) can cascade into significant weather pattern shifts (Cunico et al., 2024; Shen, 2025).

Thus, as urbanization and deforestation fundamentally alter the flow regime by increasing peak discharge and decreasing the time-to-peak, they in turn serve to intensify the forcing energy on the river's dissipative structure. This intensification often pushes the system towards geomorphic bifurcation points, where the linear relationship between flow and channel form breaks down, potentially triggering a transition from stable states (single-thread meandering) to unpredictable, multi-thread configurations (Pattison & Lane, 2012; Singh et al., 2018). A critical mechanism in this process is the disturbance-resistance feedback loop, where the balance between vegetation root resistance and flood-induced bed scour governs channel stability. The Ecomorphodynamic modeling suggests that when LULCC-driven urbanization increases flood magnitudes while deforestation reduces root anchoring, the system often follows a period-doubling route to chaos. In this state, the riverbed configuration becomes unpredictable within as few as 2 to 4 growth-flood cycles (Cunico et al., 2024).

In recent decades, concepts from non-linear dynamic systems theory, including notions of chaos and self-organization, have been increasingly recognized as valuable approaches in geomorphology for understanding and modelling the evolution and characteristics of landscapes and bedforms (Lane and Richards, 1997). This has resulted in a shift from focusing solely on equilibrium or steady-state assumptions, recognizing instead that river systems often display complex behaviours stemming from non-linear

* Corresponding author.
E-mail address: dauda.suleman@ucc.edu.gh (S. Dauda).

http://dx.doi.org/10.4314/gjg.v17i3.3

interactions between flow, sediment, and boundary conditions. As a consequence, such concepts have been increasingly applied in geomorphological research, particularly in studies of river network dynamics and channel evolution (Hooke, 2023). Notably, remote sensing has transformed fluvial geomorphology by providing abundant data for mapping, measuring, and analysing river channel changes as well as planimetric dynamics and temporal changes at wider spatial scales (Boothroyd et al., 2025). The difficulty, however, arises from the fact that many of the underlying processes driving river evolution, such as the interaction of flow, sediment, and vegetation, are non-linear, meaning that the relationship between these components and their influence on how rivers change is not simple or directly proportional (Cunico et al., 2024). Instead, these interactions involve complex feedback loops where changes in one component can have disproportionate or unexpected effects on the others and the overall system behaviour.

The Ankobra River in Ghana is a vital resource, supporting diverse ecosystems and human populations. However, the river basin has been subjected to increasing pressures from various sources, including deforestation for agricultural expansion, and particularly mining activities. These activities have the potential to significantly alter the river's hydrological regime, sediment dynamics, and overall channel morphology. Considering the growing evidence that river morphodynamics and associated processes can demonstrate characteristics of non-linearity and chaos, it becomes essential to examine in detail how land-use and land-cover changes (LULCC) interact with and alter the very conditions that drive these unpredictable and dynamic behaviours. This interplay not only intensifies the complexity of river systems but also underscores the importance of adopting integrated management strategies.

In this study, we examine the extent to which river morphology can be predicted based on LULCC as chaotic systems. Specifically, we seek to: 1) quantify the historical and current LULCC patterns and their primary driving factors in sections of the Ankobra basin; and 2) assess the direct impacts of identified LULCCs on key river morphological components, including channel width and sinuosity. In this study, we operationalize the concepts of deterministic chaos and unpredictability by treating the Ankobra River as a forced, dissipative system where LULCC acts as the primary external forcing function. To achieve the first objective of quantifying LULCC patterns, we identify anthropogenic pressures—specifically gold mining and deforestation—that serve as perturbations to the river's initial conditions. In the second objective, we assess the morphological response by utilizing channel width and sinuosity as state variables to reconstruct the river's dynamic phase space. In this context, deterministic chaos is defined not as random instability, but as aperiodic behaviour governed by nonlinear fluvial processes that exhibit a sensitive dependence on these LULCC perturbations.

Chaos is conceptualized not just as a mathematical equation, but as divergent versus convergent evolution (increasing vs. decreasing irregularity) in landforms and landscapes (Phillips, 2006). In geomorphic systems, therefore, the "Butterfly Effect" is empirically manifested when infinitesimal initial variations such as small changes in land use produce disproportionately large or long-lived morphological shifts amplified over time into macroscopically different patterns. Thus, by tracking sinuosity and width over multiple decades, the study identifies whether the Ankobra is experiencing increasing irregularity (divergence) or decreasing irregularity (convergence) as these variables are not just descriptive markers but system state variables used to reconstruct the river's phase space (Giri & Devercelli, 2023). Again, by using multitemporal satellite imagery at a scale defined by the whole Ankobra reach, it is possible to observe system-scale stationarity versus local-scale instability. This allows to test whether morphological changes are triggered by LULC changes (allogenic) or natural (autogenic or inherent chaotic migration) (Boothroyd et al., 2025; Langat et al., 2019).

This study provides an invaluable framework for monitoring, planning, and maintaining natural resources, by supplying current and extensive data on surface conditions essential for proper management (Boothroyd et al., 2025). Crucially, it contributes to the understanding of river morphodynamics, including the causes and scale of erosion and accretion, channel migration, sedimentation, and changes in river width, directly impacting aspects like the stability of riverbanks (Church and Ferguson, 2015). The insights gained are fundamental in developing flood risk management strategies, and restoration efforts aimed at sustaining ecosystem health and biodiversity, especially given the hydrological regime's influence on ecological systems. Furthermore, it allows for the advancement of geomorphic theory by providing empirical data to test and refine concepts of change while supporting the attainment of Land Degradation Neutrality (LDN) and the SDGs 6, 11, 13, and 15. By integrating remote sensing techniques, GIS analysis, and concepts from chaos theory, this research sought to provide new insights into the complex interplay of factors driving river evolution in a tropical river system facing significant environmental pressures. Understanding the role of chaotic dynamics can provide crucial insights into river evolution's inherent unpredictability and inform more effective management and restoration strategies. A study focusing on LULCC within the Ankobra basin over 3 decades is highly relevant for the appreciation of the dynamic evolution of natural resource systems and the extent of their predictability, which are the basis of effective management and policy formulation.

Materials and Methods

Study design

In geomorphological research, identification of deterministic chaos traditionally relies on quantifying sensitive dependence on initial conditions through metrics such as phase space reconstruction, correlation dimensions, and the calculation of a positive maximum Lyapunov exponent (Frascati & Lanzoni, 2010; Giri & Devercelli, 2023). While these metrics provide rigorous proof of chaos, their application requires high-frequency and continuous time-series data. Given the decadal scale and the temporal resolution of the satellite imagery used in this study (Landsat), its methodology is primarily exploratory. Essentially, it seeks to integrate remote sensing techniques and GIS analysis with these theoretical concepts to provide new insights into the Ankobra River's evolution. While the study leverages the conceptual framework of chaos—specifically the "Butterfly Effect"—to understand the river's inherent unpredictability, it also acknowledges the limitations of demonstrating formal chaos using available historical data (Hooke, 2023; Phillips, 2006).

This study, therefore, employs a quantitative approach centred on a case study of the River Ankobra in Ghana. This approach was employed to intensely explain the mechanisms generating the observed patterns in the different sections of the Ankobra in an extensive investigation. Case study design allows for deep exploration of specific events to illuminate general theoretical principles (Yin, 2016; Amofa-Appiah, 2019). While critics question its generalizability, it is important to note that with case study, meaningful insights stem from robust theoretical reasoning rather than empirical extrapolation. An understanding of river system behaviour thus, depends on examining nonlinearity in each unique context, a task that can best be accomplished through a quantitative approach.

Study area

The Ankobra River Basin is a significant hydrological system located in the southwestern part of Ghana. Specifically, it is situated between latitudes 4°52′–6°27′N and longitudes 1°42′–2°33′W (see Figure 1). The river itself is approximately 190 km (120 miles) long, taking its source from the Bibiani Hills (or Bebianiha mountain ranges near Sefwi Anwiaso) at an altitude of 368m or 549m, respectively. It flows southwards, discharging into the Gulf of Guinea (Atlantic Ocean) at Sanwoma (Asare et al., 2019). The total catchment area of the Ankobra Basin varies slightly across sources, reported as 8,272 km², 8,366 km², 8,403 km², 8,793.00 km², and approximately 9,000 km². It spans across parts of the Western and Central Regions of Ghana, including districts like Wassa Amenfi, Wassa West, and Nzema East and its major tributaries include the Manse, Fure, Bonsa, Bonsaso, and Asuo Kofi. Topographically, the region is generally low-lying and predominantly undulating; with over 80% of its landmass below 14m above sea level (Osman et al., 2016).

The Ankobra Basin falls under the equatorial rainforest or wet semi-equatorial climatic zone characterized by a warm (25 to 30 °C), humid (64-95%) climate, with temperatures ranging between 21 °C and 32 °C. The basin experiences a bimodal rainfall pattern, with two distinct rainy seasons: a heavy rainy season from April to June (or May-August) and a light rainy season from September to November (or September-October). Annual precipitation in the basin ranges from 1,200–2,200 mm or 1,300 mm to 2,000 mm, making it the wettest climatic region in Ghana with mean annual rainfall

above 1,900 mm (Affum et al., 2024). The Ankobra Basin is one of Ghana's main mining regions, with extensive mining, agricultural, and urban development activities taking place in various locations. Arsenic hotspots have been identified in known gold-mining areas like Nzema, Obuasi, Prestea, and Tarkwa. The region hosts several large-scale gold mines (Affum et al., 2024; Awuah, 2016.) around Prestea, Tarkwa, Iduaprim and Damang), and numerous small-scale ventures and illegal artisanal mining (locally called "galamsey") operations. These mining activities contribute significantly to environmental pollution, including heavy metals like mercury, lead, arsenic, and cadmium in river sediments and water (Asare et al., 2019).

Data source

The primary data used for this study are Landsat imaging scenes obtained from the freely accessible data portal of the United States Geological Survey (USGS) (see: http://earthexplorer.usgs.gov/). The Landsat program is a significant resource for monitoring river geomorphology due to its archive length, providing data from the 1970s onward with predictable time intervals for acquisition (Boothroyd et al., 2025). The specific Landsat images selected for analysis are presented in Table 1.

Data Processing and Analysis

The raw satellite images obtained from the United States Geological Service (USGS) portal required some pre-processing steps to ensure their quality and suitability for classification. The ENVI 5.3 software was therefore, used to perform such operations including radiometric calibration, atmospheric correction, and image enhancement. These steps are crucial for removing distortions caused by atmospheric conditions and sensor characteristic. Pre-processing helps in making the satellite data more suitable for analysis by correcting errors and improving visual interpretability or digital analysis.

Following pre-processing, the satellite images for each period (1991, 2001, 2010, and 2024) were subjected to LULC classification using ENVI software. LULC classification involves assigning pixels in the satellite imagery to predefined categories that represent different types of land use or land cover, such as vegetation, urban structure (built-up areas), bare soil, or water bodies. To evaluate the reliability of the generated LULC maps, an accuracy assessment was conducted. This process involves comparing the classified map to a reference dataset representing the 'ground truth'. In this study, Google Earth Pro served as a reference source for visual verification and accuracy assessment. This allowed for checking whether areas classified on the satellite image (using ENVI) corresponded correctly to their appearance in the high-resolution imagery available through Google Earth Pro. Accuracy assessment typically involves calculating metrics such as overall accuracy, producer's accuracy, user's accuracy, and the Kappa coefficient.

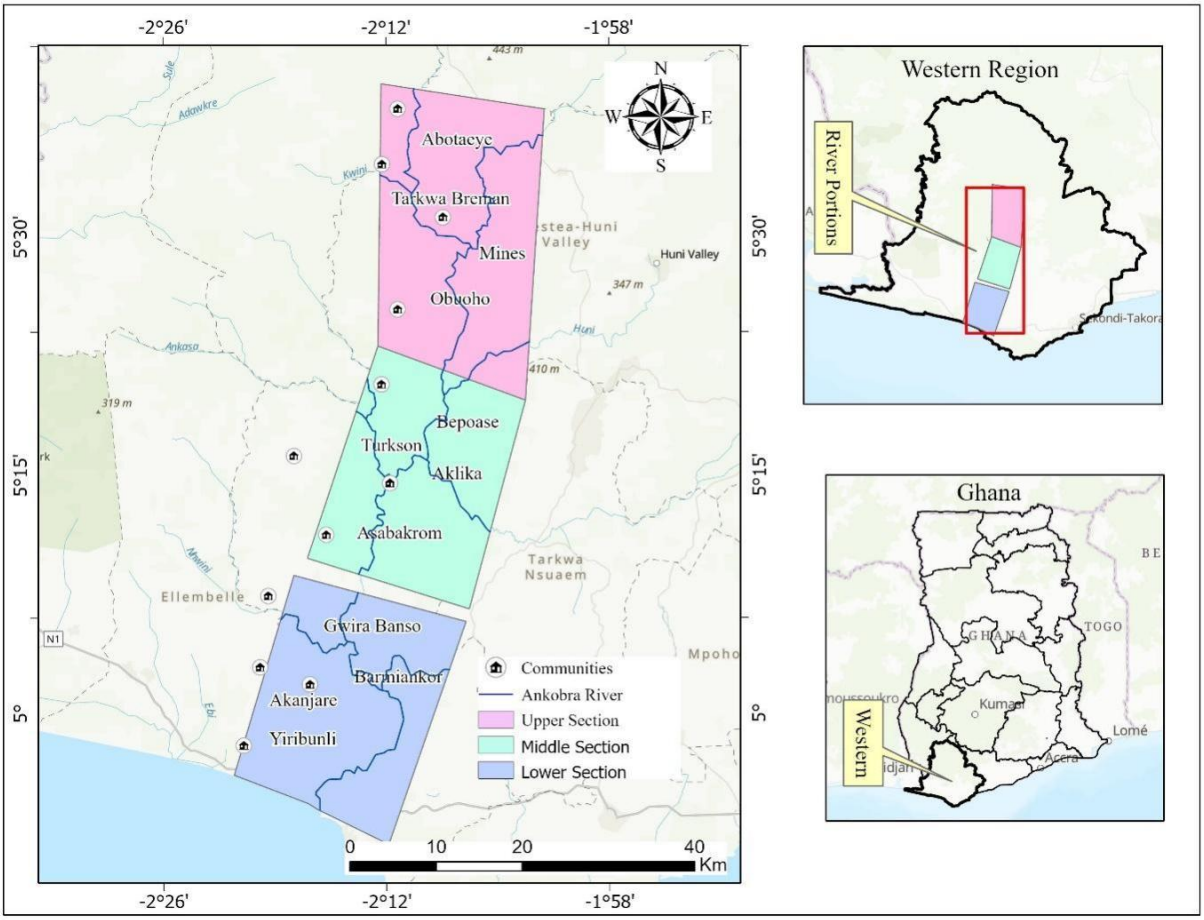

Figure 1: Map of the study area
Source: Ghana Shapefile

Table 1: Landsat Images

Satellite Data	Acquisition Date	Sensor	Spatial Resolution	Collection Level	Tier
Landsat 5	01/01/1991	TM	30 meters	C2L2	1
Landsat 7	04/02/2001	ETM+	30 meters	C2L2	1
Landsat 8	01/03/2010	OLI	30 meters	C2L2	1
Landsat 9	12/21/2024	OLI	30 meters	C2L2	1

Source: USGS

Once the LULC maps for different years were classified and validated, spatio-temporal analysis was conducted to quantify and characterize the changes in LULC patterns within the Ankobra River basin over the 30-year study period. This involved comparing the LULC maps from different years to identify areas where the land cover type changed. The resulting LULC change information was then used in conjunction with the quantified changes in the river channel's width and sinuosity to explore the relationships among these dynamic aspects of the river system.

Image classification

Image classification helps to identify and classify image features based on their representation on the ground or earth surface. In remote sensing, image classification can be supervised or unsupervised. To categorize the satellite images, a supervised classification approach, specifically the support vector machine classifier, commonly known as SVM, which is popular due to its ease of use and training, was used. This approach classifies satellite image pixels based on their chance of belonging to a given land use and land cover class. The spectral signature of each picture pixel was compared to training samples from the research region, and satellite images were categorized into four broad land use/land cover (LULC) categories: built-up areas, sparse vegetation, dense vegetation, and water as outlined in Table 2. Based on the USGS land cover Classification Scheme, these classes were selected on the basis of their direct relevance to river morphology:

- Water: Essential for extracting the river's geometry and analyzing changes in width and sinuosity.
- Dense Vegetation: Crucial for stability, high canopy cover and root reinforcement enhance bank stability and reduce surface runoff.
- Sparse Vegetation: Associated with grassland or degraded land, these areas are susceptible to erosion, often leading to increased sediment input and channel widening.
- Built-up Areas: Although often occupying a small area, impervious surfaces significantly alter hydrological processes by increasing runoff and accelerating sediment transport, which drives channel instability.

To classify the satellite images, 10 training samples were generated using the Envi 5.6 software (region of interest) tool for each of the classes. The software facilitated effective classification of land use and land cover spectral classes. In addition, Google Earth Pro was used to create validation samples. These samples were used for accuracy assessments to ensure that what was classified on the image was an accurate representation of itself on the ground.

Extraction of Morphological Metrics: Width and Sinuosity

The quantification of river morphological components—specifically channel width and sinuosity—was achieved through a vector-based analytical approach derived from the classified LULC maps. This process followed a three-stage workflow:

Channel Delineation and Vectorization

Following the supervised classification of the multi-temporal satellite imagery, the resulting raster datasets were converted into vector format using the Raster to Vector tool in ArcGIS Pro. The "Water" class was isolated and extracted to represent the active river channel for each study year. A river centerline was generated along the flow direction to serve as a baseline. Perpendicular transects were then created at 90˚ angles from this line at 300-meter intervals. To ensure accuracy, the extracted vector layers were manually inspected and refined to maintain channel continuity and eliminate misclassified noise that did not form part of the primary river course.

Channel Width Quantification (Transect Method)

Channel width was quantified at the spatial resolution of the original satellite imagery (30m for Landsat) to ensure consistency. Width was measured in ArcGIS Pro as the distance between the left and right banks intersected by these transects. While numerous transects were initially generated across both straight and meandering sections, a subset of 20 transects was selected for each section (upper, middle, and lower) to maintain representative coverage while reducing potential redundancy or measurement error. The average width for each section and period was calculated by summing all selected transect measurements and dividing by the total number of transects.

Sinuosity Calculation

Sinuosity (Si) was calculated as the ratio of the river's actual path to its shortest possible path. Thus, it was quantified using a standard geometric approach:

Sinuosity = Channel Length/Straight-Line Distance.

Channel Length (Cl), measured as the total length along the extracted river centreline, and valley Length (Vl), measured as the straight-line distance between the upstream and downstream endpoints of each defined basin section (Upper, Middle, Lower). Width and sinuosity measurements were conducted at the original spatial resolution of the satellite imagery used for the LULC classification, ensuring consistency between the source data and the derived parameters.

Figure 2 summarizes the methodological flow chart employed in the study.

Table 2: Land use Land cover description

	Land use land cover types.	Description
1	Built-Up Areas	These are areas are the various places or areas that have undergone major changes due to the activities of human and infrastructural development. These places are usually denoted by high-density structures which include residential, commercial, industrial, and institutional buildings among others.
2	Dense Vegetation	Dense vegetation refers to areas with high plant cover and thick foliage, meaning the ground is mostly or entirely covered by vegetation. These areas typically have a high Normalized Difference Vegetation Index (NDVI), indicating a healthy and rich plant presence.
3	Sparse Vegetation	Sparse vegetation refers to areas with low plant cover, where the ground is partially or mostly exposed due to scattered or minimal vegetation. These areas have a lower NDVI, indicating a reduced plant density.
4	Water Bodies/Rivers	Water bodies and rivers refer to all surface water features, whether natural or man-made. This category includes rivers, lakes, ponds, reservoirs, and coastal waterways.

Source: USGS Anderson Land Cover Classification Scheme

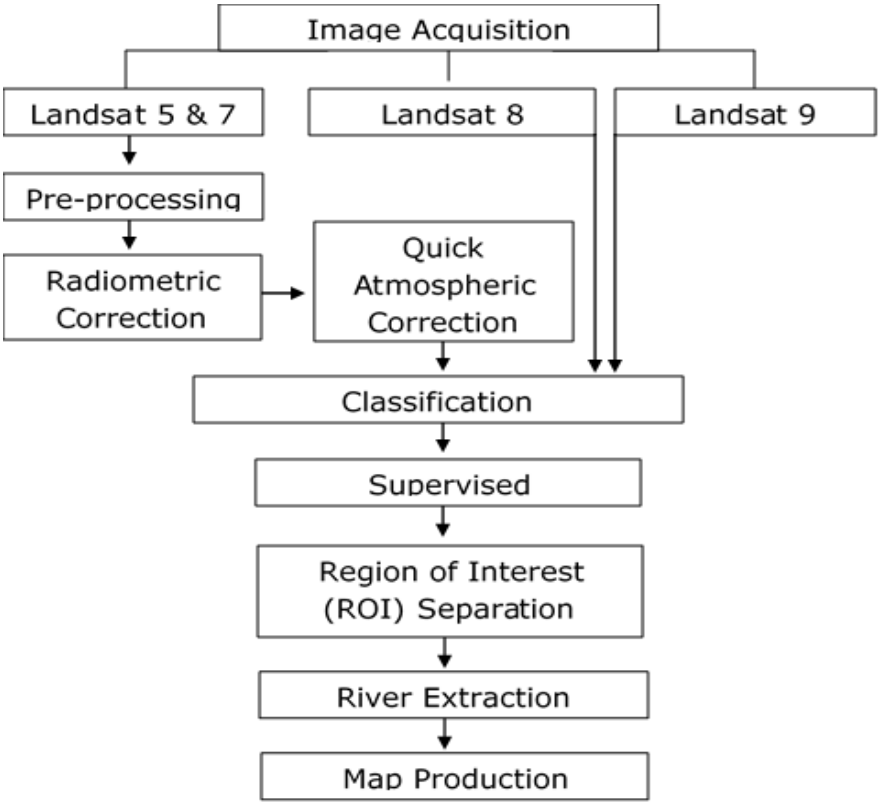

Figure 2: Methodological Framework Flow Chart

Results

Quantification of Historical and Current LULCC Patterns and Driving Factors

This section presents the findings related to the quantification of LULCC patterns in the three sections of the Ankobra river basin and their driving factors. Four major land use land cover classes including water, dense vegetation, sparse vegetation and built-up were identified in all the sections. Figure 3 and table 3 present the results of the classification in the lower section of the river.

As indicated in Figure 3, the lower section of the Ankobra basin recorded an increase in water class from the base year to 2001, where from occupying about 0.54% in the lower basin, it increased to occupy an area of about 0.88% in 2001. However, there was a drastic drop by 2024 to about 0.31%. Similarly, both the sparse vegetation and built-up classes also increased in areas in 2021 from the base year. While there was a decline in sparse vegetation in 2024, the area of built-up land rather increased from 0.78 % in 2001 to 1.02% in 2024. Nonetheless, the dense vegetation class which occupied the largest area in the lower section of the Ankobra river in the base year decreased in 2001 from 29.38% to 20.04% and increased to about 22.5% in 2024. The accuracy of the LULC classifications was evaluated separately for each study year and river section to account for spatial variability and Table 4 summarizes the accuracy assessment derived for the lower section:

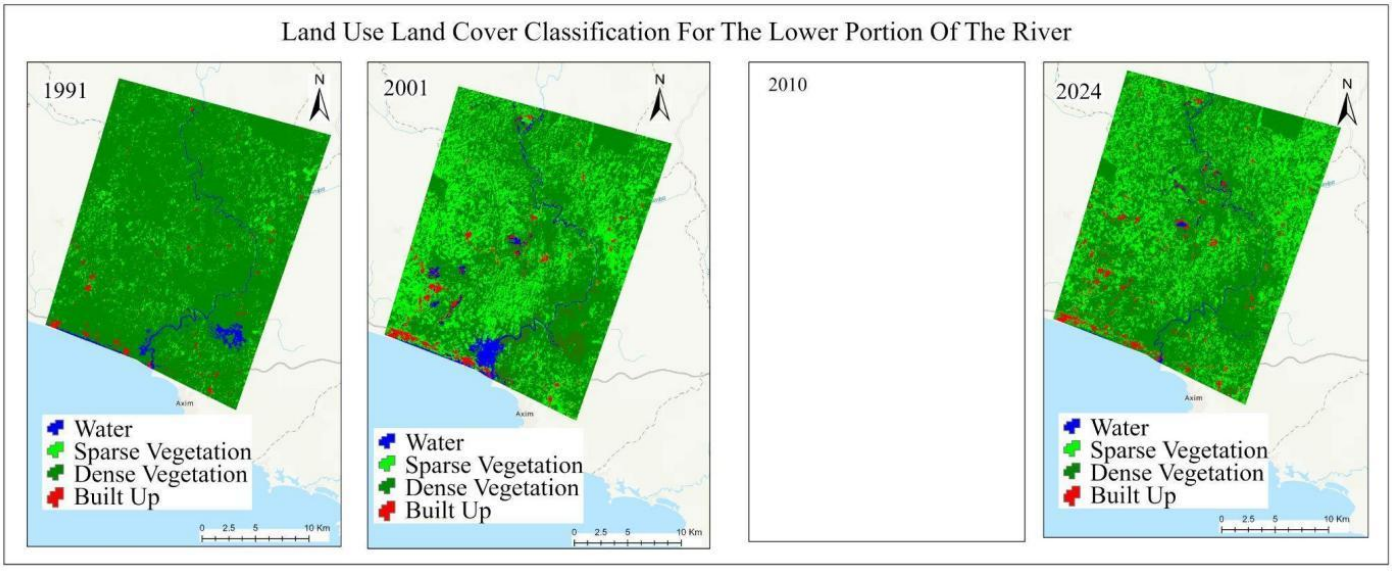

Figure 3: LULC Classification for the Lower Section of the Ankobra River

Table 3: Areal Estimations of LULC Classification in the Lower Section of Ankobra and their Percentage Change

Class	Area (1991) km^2	%	Area (2001) km^2	%	Area (2024) km^2	%
Water	8.49	0.54	13.92	0.88	4.95	0.31
Dense Vegetation	464.73	29.38	316.97	20.04	355.92	22.50
Sparse Vegetation	34.75	2.20	149.31	9.44	136.59	8.64
Built Up	5.7	0.36	12.37	0.78	16.2	1.02
Total	513.67		492.57		513.66	

Table 4: Accuracy of the Land Use and Land Cover (LULC) classifications for each year in the Lower section

Year	Overall Accuracy (%)	Kappa Coefficient
1991	94.17	0.91
2001	93.33	0.9
2010	93.33	0.9
2024	91.67	0.88

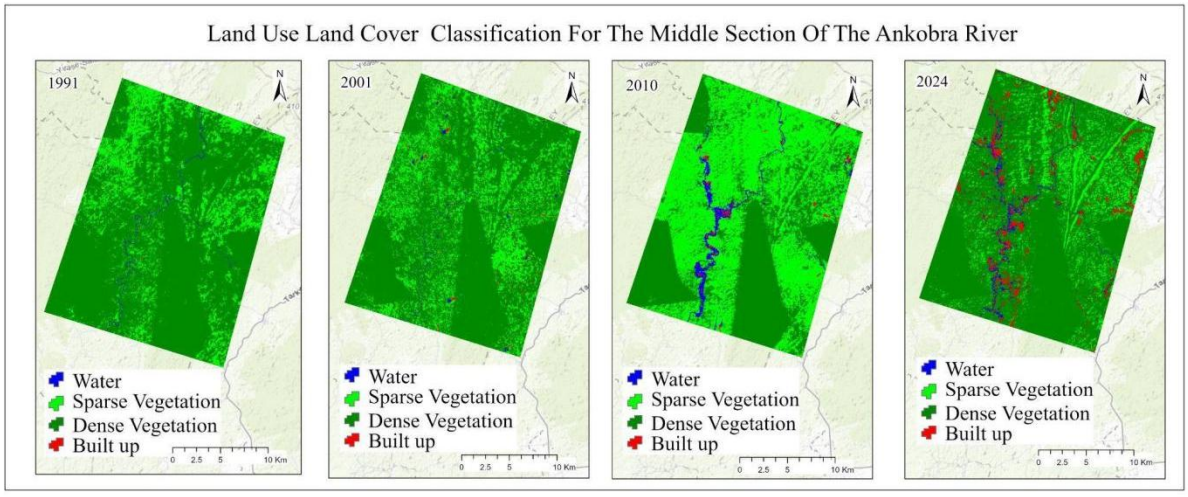

Figure 4: LULC Classification for the Middle Section of the Ankobra River

Table 5: Areal Estimations of LULC Classification in the Middle Section of Ankobra and their Percentage Change

Class	Area (1991) km^2	%	Area (2001) km^2	%	Area (2010) km^2	%	Area (2024) km^2	%
Water	2.72	0.17	3.43	0.22	12.96	0.82	9.62	0.61
Dense Vegetation	400.38	25.31	378.74	23.94	216.84	13.71	292.27	18.48
Sparse Vegetation	79.64	5.03	96.98	6.13	239.45	15.14	160.39	10.14
Built Up	0.38	0.02	3.97	0.25	4.86	0.31	20.84	1.32
	483.12		483.12		474.11		483.12	

In the middle section, the findings, as presented in Figure 4 and Table 5 reveal that LULC classes are the same as in the lower section in terms of water, sparse vegetation, dense vegetation and built-up.

In the middle section, the dominant land cover class in the base year was dense vegetation, covering an area of about 25.32%, and with built-up being the class with the least area of 0.02%. However, over the subsequent two decades (2001) and (2010), as presented in Figure 4, dense vegetation class reduced in area to 23.31% and 13.71% respectively, while built-up increased over 2001, 2010 and by 2024, it occupied an area of about 1.32%. Sparse vegetation and water also increased in their respective areas in 2001 and 2010 respectively, but declined in 2024. Thus, from occupying an area of 15.14% in 2010, the area of sparse vegetation reduced to about 10.14% while water decreased from 0.82% in 2010 to 0.61%. Accuracy assessment was evaluated using reference samples generated via the ArcGIS Pro Create and the validation points were entirely independent of the training data to minimize bias. Table 6 presents the accuracy assessment for the middle section.

Table 6: Accuracy of the Land Use and Land Cover (LULC) classifications for each year in the Middle section

Year	Overall Accuracy (%)	Kappa Coefficient
1991	96.67	0.96
2001	94.17	0.92
2010	93.33	0.91
2024	92.5	0.9

Figure 5 and Table 7 present the findings in LULC classes with the same classification used in the lower and upper sections of the Ankobra river.

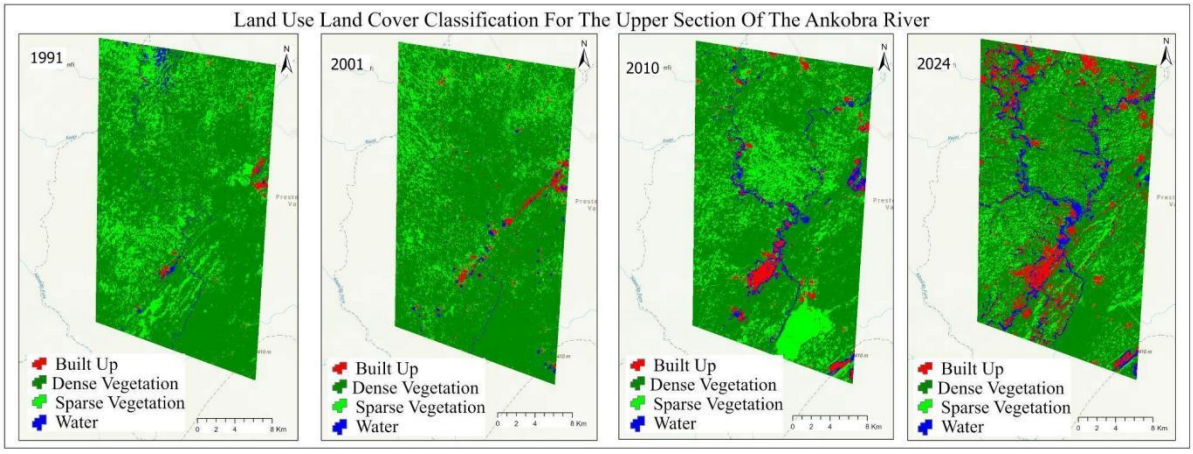

Figure 5: LULC Classification for the Upper Section of the Ankobra River

Table 7: Areal Estimations of LULC Classification in the Upper Section of Ankobra and their Percentage Change

Class	Area (1991) km^2	%	Area (2001) km^2	%	Area (2010) km^2	%	Area (2024) km^2	%
Water	7.09	0.44	10.3	0.65	18.93	1.20	27.24	1.72
Dense Vegetation	474.67	30.0	480.76	30.39	428.94	27.12	404.42	25.57
Sparse Vegetation	98.47	6.22	81.06	5.12	116.15	7.34	89.95	5.69
Built Up	4.74	0.30	12.84	0.81	20.94	1.32	63.36	4.01
	584.97		584.96		584.96		584.97	

Unlike the lower and the middle sections of the river, the water area of the upper section of the Ankobra River recorded a consistent increase from 0.44% in the base year (1991) to 0.65% by the end of the study period (2024). Dense vegetation recorded a steady decrease after 2001 as compared to the spare vegetation which showed some form of fluctuation from 1991 to 2024. Built-up area recorded a significant increase in area from 0.30% in 1991 to 4.01% in 2014. The overall accuracy for the upper section was 100%, implying the model perfectly predicted the land use/land cover classes in the validation dataset. The reported 100% accuracy in the upper river section reflects the dominance of spectrally distinct and spatially homogeneous land cover classes—specifically dense vegetation and water—which results in high class separability. Again, to ensure that this high score was not an error, the validation dataset was specifically re-examined to confirm its independence from training samples. However, this result is interpreted with caution, acknowledging that it may be influenced by landscape simplicity and the specific size of the validation sample and Table 8 presents the accuracy assessment for the upper section.

Table 8: Accuracy of the Land Use and Land Cover (LULC) classifications for each year in the Middle section

Year	Overall Accuracy (%)	Kappa Coefficient
1991	100	1
2001	97.5	0.97
2010	96.67	0.96
2024	95.83	0.94

Based on the maps and tables, it could be observed that the driving factors influencing land use land cover changes in the Ankobra basin are deforestation and urbanization.

Direct impacts of identified LULCCs on key river morphological components

This section details the observed and modelled direct impacts of LULCCs on key river morphological components, specifically channel width and sinuosity, within the different sections of the Ankobra basin during the 1991-2024 study period. The analysis integrated data from remotely sensed multi-temporal satellite imagery alongside findings from the relevant hydrological and morphodynamic models within a Geographical Information Systems (GIS).

In the transition matrix tables, row headers represent the LULC classes at the start of the period, while column headers represent the classes at the end of that period. Diagonal values in the tables indicate areas (in km²) that remained unchanged within their respective LULC categories. Off-diagonal values, on the other hand, show the area of land (in km²) that significant transformations occurred. Table 9 below presents the transition matrix of the lower section between the periods of 1991-2001, and 2010-2024.

Thus, within 1991-2001, the areas of built-up, dense vegetation, sparse vegetation, and water that remained unchanged were 3.17, 306.65, 18.76 and 4.82 km^2 respectively. Major transformations in this period were mainly from dense vegetation to sparse vegetation, water and built-up. However, within 2010-2024, the area of built-up, which maintained increased to 8.32km^2, while dense vegetation experienced a drastic decline to 3.32km^2 in the lower section of the Ankobra basin. Areas of sparse vegetation and water also declined within 2010-2024. Nonetheless, the transformation patterns were different, with a rather greater portion of the dense vegetation being transformed into sparse vegetation between 2010-2024. However, the decline in the area's sparse vegetation was due to transformations into built-up mainly. Comparing the total gains and losses in the LULC classes, it can be seen from Table 9 that, at the end of 2001, the areas of built up and water increased while that of dense vegetation and sparse vegetation decreased drastically. However, at the end of the period between 2010 and 2024, there was a drastic increase in the area of built-up and sparse vegetation contrary to that of the dense vegetation and waters.

River channel width is a typical ecological metric used to calculate properties such as water discharge rates and, applied generally in hydrological and ecological monitoring. According to Scherelis et al. (2023), previous ecological works of river channel width measurements have been successful based on in situ measurements or remote sensing efforts. However, the authors contend that they poorly captured river width variability due to simplifications of the river network or due to the sparse availability of in situ measurements. The findings in Table 10, therefore, apply remote sensing, geospatial processing, and descriptive statistics (standard deviation) to capture channel width variability, necessary to study the temporal changes of the Ankobra river properties, as suggested by Scherelis et al. (2023).

Table 9: Transition Matrix of the Lower Section

		1991-2001	(km^2)		
	Built-Up	Den. Veg.	Spar. Veg.	Water	Total
Built-Up	3.17	0.94		0.15	0.15
Den. Veg.	8.19	306.65	126.32	8.67	449.83
Spar. Veg.	0.83		18.76	0.29	449.98
Water	0.05	0.16	0.1	4.82	5.13
Total	12.24	0.16	145.18	13.93	

		2010-2024	(km^2)		
Built-Up	8.32	1.66		2.23	2.23
Den. Veg.	0.06	3.52	263.56	0.75	267.89
Spar. Veg.	64.08		79.56	0.12	270.12
Water	0.62	9.79	0.16	3.38	13.95
Total	73.08	9.79	343.28	6.48	

Table 10: Average changes in channel width of the Lower section

Year	Section	Avg_Width	Std_Ddev	%Change	Sinousity
1991	Lower	98.08	50.52	-	1.895
2001	Lower	104.38	63.34	6.4	1.885
2010	Lower	97.1	25.81	-1.00	1.879

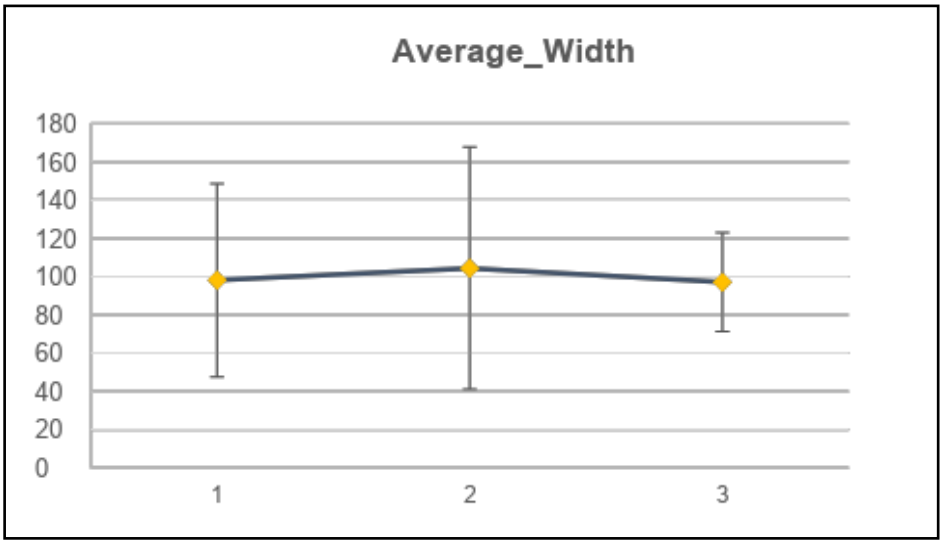

Figure 6: Average changes in channel width of the lower section

In Figure 6, the average channel width of the lower section of the Ankobra river exhibited a change over the study period. The average width in 1991, recorded at 98.08 meters, expanded to 104.38 meters by 2001, representing a 6.4% expansion from the 1991 measurement. This expansion details that the lower section of the river experienced erosional processes or increased flow energy, leading to the lateral widening of its channel (Whitbread, et al. 2015). Figure 6 visually depicts this upward trend from point 1 to point 2, illustrating the channel's outward adjustment. Subsequently, the periods of 2001 and 2024, experienced a slight narrowing in average width to 97.1 meters, which is a -1.00% reduction from the 1991 baseline, signalling that the channel is adjusting towards a new, slightly narrower equilibrium, depicted by the line on the chart from point 2 to point 3 (Whitbread, et al. 2015). River width can greatly vary and change over space and time, complementing the temporal expansion and narrowing in the findings above. The width variability in the lower section of the Ankobra River is common due to its importance in sediment bar dynamics (Scherelis et al., 2023).

Concurrently, the standard deviation also increased from 50.52 meters in 1991 to 63.34 meters by 2001 indicating non-uniform channel widening along the entire lower section. In river systems, standard deviation of channel width is a measure of how much the width varies across a specific reach or channel. A larger standard deviation indicates greater variability in width, meaning the channel is more irregular in shape, while a smaller standard deviation suggests a more uniform width (Dong & Goudge, 2022). Therefore, the increase in standard deviation between the periods of 1991 and 2001 implies increased heterogeneity of more pronounced erosion and expansion within this segment, reinforced by the large error bar around point 2 in Figure 6. Again, a significant reduction in standard deviation from 63.34 meters in 2001 to 25.81 meters in 2024 signifies a more uniform and less variable channel width across the lower section by the end of the study period despite the minor overall average width change. This is depicted in the diagram with a smaller error bar around point 3 in Figure 6, suggesting reduced spread.

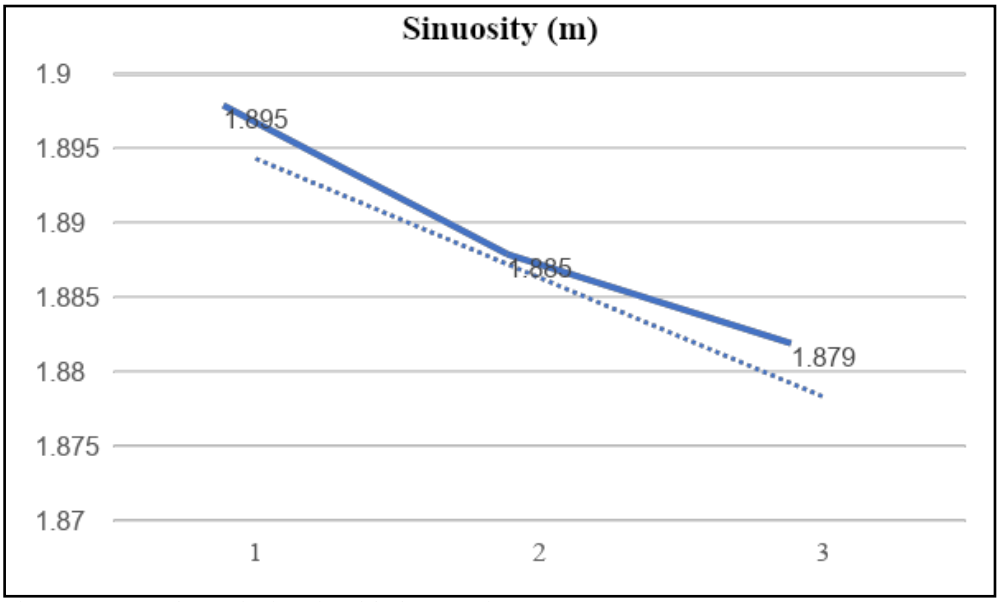

Figure 7: Average changes in sinuosity of the lower section

Table 11: The transition matrix of the middle section between the periods of 1991-2001, 2001-2010, and 2010-2024

		1991-2001	Km2		
	Built-Up	Dense Veg.	Sparse Veg.	Water	Total
Built Up	0.17	0.07	0.12	0	0.36
Dense Veg.	2.5	332.77	65.71	1.05	402.03
Sparse Veg.	1	46.72	30.02	0.31	402.39
Water	0	1.47	0.12	1.03	2.6
Total	3.67	381.03	95.97	2.39	
		2001-2010	Km^2		
Built Up	0.43	0.9	2.32	0.08	3.73
Dense Veg.	2.19	190.22	178.89	9.59	380.89
Sparse Veg.	0.99	24.44	68.66	1.99	384.62
Water	0.16	0.27	0.64	1.29	2.36
	3.77	215.83	250.51	12.95	
		2010-2024	Km^2		
Built Up	2.39	0.93	0.14	0.33	3.79
Dense Veg.	4.1	198.06	11.21	2.5	215.87
Sparse Veg	11.27	190.28	46.62	2.29	219.66
Water	2.7	5.76	0.2	4.27	12.93
	20.46	395.03	58.17	9.39	

As highlighted in Figure 7, the sinuosity values for the lower section of the Ankobra River displayed a consistent, albeit minor, decreasing trend across the observed periods. The values provide insights into the platform evolution of the river, starting at 1.895 in 1991, and slightly decreased to 1.885 by 2001. This gradual reduction continued, with the sinuosity recorded as 1.879 in 2024. The initial sinuosity value of 1.895 in 1991 indicates that a highly meandering platform characterized the lower section of the Ankobra River, as a significant value > 1.5 indicates meandering (Sukarno, et al. 2019). Consistently, albeit minor, the decreasing trend in sinuosity from 1.895 in 1991 to 1.885 in 2001, and further to 1.879 by 2024, reveals a subtle but persistent tendency towards channel straightening or a reduction in the river's overall tortuosity over the study duration (Sukarno, et al. 2019). Figure 7 visually reinforces this trend, showing a gentle, continuous downward slope across the three points, illustrating the subtle but persistent reduction in the river's meandering character. While the magnitude of change is small, its consistency over decades can be geomorphologically significant. Besides, the gradual straightening could be a response to low sediment discharge, a potential cause highlighted in the literature (Petrovszki et al., 2014).

From Table 11, the areas of built-up, dense vegetation, sparse vegetation, and water that remained unchanged were 0.17, 332.77, 30.02, and 1.03 km^2, respectively. Major transformations in this period were mainly dense vegetation into sparse vegetation (65.71 km^2), sparse vegetation to dense vegetation (46.72 km^2), and water to dense vegetation (1.47 km^2). Consequently, in comparing the gains and losses of this period, except built-up which increased from a total of 0.36 km^2 at the end of 1991 to a total of 3.67 km^2 at the end of 2010, all the other land use classes experienced some loses with the drastic one being sparse vegetation, from 402.39 km^2 at the end of 1991 to 95.9 km^2 by 2001.

However, between 2001 and 2010, the area of built-up that maintained increased to 0.43 km^2, while dense vegetation decreased to 190.22 km^2 in the middle section of the Ankobra basin. Areas of sparse vegetation that maintained increased to 68.66 km^2 and that of water, also increased to 1.29 km^2. Major transformations within this period were that from dense vegetation to sparse vegetation 178.89 km^2 and dense vegetation to built-up (2.19 km^2). However, in terms of net gains and losses, the area of water gained significantly in 2010 compared to its area in 2001, increasing from 2.36 km^2 to 12.95 km^2. In the case of built-up, even though there was a net gain, it was not significant (from 3.73 km^2 to 3.77 km^2 respectively) as compared to the previous period between 1991 and 2001.

In the period between 2010 and 2024, the area of built-up area that remained unchanged was 2.39 km^2, while that of dense vegetation was 198.06 km^2. The sparse vegetation and water were 46.62 km^2 and 4.27 km^2, respectively. Compared with that of the previous period (2001-2010), the area of sparse vegetation decreased, unlike the other three classes, which increased their areas, and remained unchanged. Such a drastic decline in the area of sparse vegetation could be explained by this class being transformed into less built-up (11.27 km^2) and more dense vegetation. Comparing the net losses and gains for the various classes, it can be seen from Table 11, that built-up and dense vegetation experienced net gains at the end of 2024 from 3.79 km^2 to 20.46 km^2, and from 215.87 km^2 to 395.03 km^2 respectively. Nonetheless, sparse vegetation and water experienced some net losses at the end of the period, with sparse vegetation declining from an area of 219.66km2 to 58.17 km^2 and water also losing from an area of 12.^{93} km^2 to an area of 9.39 km^2.

In the middle section of the river, the findings show that the average channel width exhibited a progressive widening over the study period. From Table 12, the average width began at 47.77 meters in 1991, then widened slightly to 47.96 meters by 2001, signalling a 0.40% change, and further to 48.57 meters by 2010, a 1.70% change from 1991. This progressive widening indicates a slow, but consistent tendency towards lateral expansion of the channel, visually depicted in blue line with the gradual upward trend in Figure 8, from point 1 to point 3, showing a relatively stable width for nearly two decades (Whitbread, et al. 2015). On the other hand, a significant change occurred between 2010 and 2024, with the average channel width substantially widening to 77.15 meters, representing a considerable (61.50%) change from the 1991 baseline. This rapid and substantial widening in the later period depicts a change in the geomorphological processes, suggesting a period of intense lateral erosion or a significant increase in the volume of water and/or sediment the channel is accommodating (Ruiz-Villanueva et al., 2023). Figure 8 visualizes the expansion with a steep upward slope of the green line from point 3 to point 4.

Concurrently, the standard deviation between the period of 1991 and 2010 initially decreased from 7.61 meters in 1991 to 6.94 meters by 2001, with a narrow reduction in the variability of the channel width during the initial period of minor widening. This is further depicted in Figure 8 with relatively small error bars for the first three points. However, it increased to 8.47 meters by 2010 and further increased to 26.59 meters in 2024. Fluctuations in standard deviation during the initial period suggest that while the channel was gradually widening, the spatial consistency of the width did not change dramatically. Conversely, a substantial rise in standard deviation between the period of 2010 to 2024 indicates a highly non-uniform significant channel widening, implying increased heterogeneity and localized areas of more extreme widening or complex morphological adjustments within this section (Baynes et al., 2020). This increased variability is visible with a larger error bar around point 4 in the Figure 8.

Sinuosity of the middle section also showed significant fluctuations throughout the observed periods. In 1991, sinuosity was recorded at 1.83 and decreased to 1.722 by 2001, suggesting a tendency towards channel straightening. Such a decrease occurs if the river's flow becomes more efficient, eroding the outer banks of meander bends or cutting across meander necks, leading to a more direct path (Kyuka et al., 2020). Subsequently, sinuosity increased to 1.856 by 2010, indicating a renewed tendency towards a more tortuous or meandering planform.

Table 12: Average changes in channel width of the middle section

Year	Section	Avg_Width	Std_Ddev	%Change	Sinousity
1991	Middle	47.77	7.61	-	1.83
2001	Middle	47.96	6.94	0.40	1.722
2010	Middle	48.57	8.47	1.70	1.856
2024	Middle	77.15	26.59	61.50	1.78

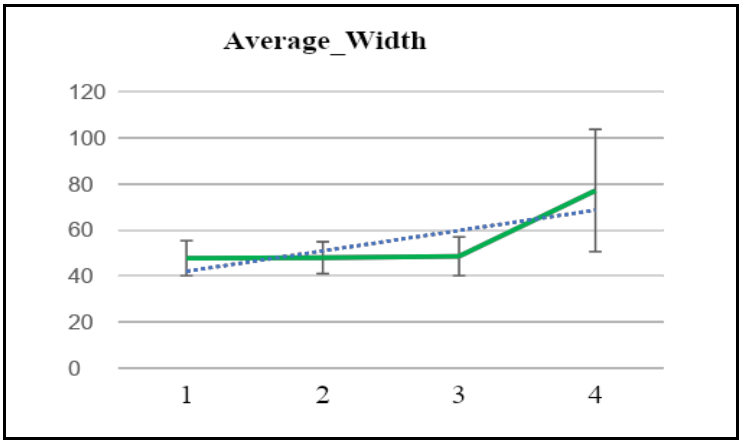

Figure 8: Average changes in channel width of the middle section

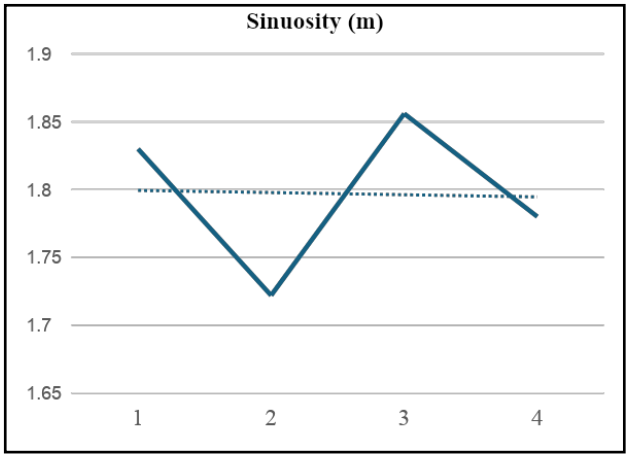

Figure 9: Average changes in sinuosity of the middle section

The increase could be a response to changes in sediment supply, flow conditions that favour meander development, or the river attempting to regain a more stable, longer course (Zhang, 2024). This is shown in Figure 9 with a sharp upward trend from point 2 to point 3, depicting an increase in meandering. Eventually, the sinuosity value in 2024 slightly reduced to 1.78 meters. This final adjustment suggests a minor tendency towards straightening again after the previous period of increased meandering.

From Table 13, most of the land cover remained stable, with 415.66 km² of dense vegetation, 25.32 km² of sparse vegetation, 2.61 km² of built-up and 0.91 km² of Water retaining their original classification. Significant transformations included 51.35 km² of dense vegetation converting to sparse vegetation, and 67.91 km² of sparse vegetation transitioning to dense vegetation. After the end of this period, built-up and dense vegetation classes experienced significant net gains by increasing from an area of 4.69 km^2 to 13.35 km2 and 477.94 km^2 to 489.61 km^2, respectively. Conversely, sparse vegetation and water classes experienced net losses from 95.55 km^2 to an area of 77.79 km^2 and 6.75 km^2 to 4.18 km^2, respectively.

Through the period of 2001 to 2010, 366.92 km² of dense vegetation, 14.5 km² of sparse vegetation, 3.62 km² of built-up and 1.35 km² of Water remained unchanged. Notable land cover changes included 97.47 km² of dense vegetation converting to sparse vegetation, and 56.25 km² of sparse vegetation transforming into dense vegetation. Additionally, 11.78 km² of dense vegetation became built-up and 13.47 km² of dense vegetation converted to water. Significant net gains at the end of this period included sparse vegetation from 77.69 km^2 to an area of 113.54 km^2, water from 4.18 km^2 to an area of 18.84 km^2, and built-up from 13.40 km^2 to an area of 20.83km^2. Only the dense vegetation class experienced a net loss from 489.64 km^2 to an area of 431.7 km^2 by the end of this period.

After the period of 2010-2024, the analysis showed 330.38 km² of dense vegetation, 30.13 km² of sparse vegetation, 12.8 km² of built-up and 10.36 km² of Water maintained their original land cover. Significant conversions included 35.52 km² of dense vegetation transitioning to built-up, and a substantial 45.8 km² of dense vegetation converting to water. Furthermore, 69.06 km² of sparse vegetation changed to dense vegetation. The end of this period also experienced notable net gains and losses. While classes of built-up and water improved with an increase from 20.9 km^2 to an area of 62.26 km^2 and 18.9 km^2 to an area of 59.28 km^2 respectively, both sparse and dense LULC classes experienced net losses of 113.84 km^2 and 431.3 km^2 to an area of 54.03 km2 and 409.34 km^2 respectively.

Average channel width in the upper section demonstrated a continuous and significant expansion from 56.34 meters in 1991, to 72.24 meters by 2001 (a 28.20% expansion), then to 114.12 meters by 2010 (a 102.60% expansion from 1991), and finally to 168.63 meters by 2024, representing a nearly 200% change (199.30%) from its initial width. This consistent and accelerating lateral expansion indicates a dominant regime of bank erosion and channel adjustment to accommodate increased energy or sediment flux (Candel et al., 2020). The fig reinforces this trend with a steep and continuous upward trajectory, illustrating a pronounced and sustained widening.

Concurrently, the standard deviation considerably increased across the study period from 14.07 meters in 1991, to 18.92 meters in 2001, 44.24 meters in 2010, and a significant 97.53 meters in 2024. This deviation signifies that the channel widening was highly non-uniform across the upper section and suggests a progressively greater spread in individual width measurements around the average, implying increased heterogeneity, localized areas of extreme widening, or the development of more diverse morphological features within this reach, as experienced in the latter period of the middle section (Baynes et al., 2020). The error bars on the chart visibly grow larger with each subsequent point, emphasising increasing variability and spatial inconsistency in channel width.

Table 13: Presents the transition matrix of the upper section between the periods of 1991-2001, 2001-2010, and 2010-2024

		1991-2001	km^2		
	Built-Up	Dense Veg.	Sparse Veg.	Water	Total
Built Up	2.61	1.03	0.69	0.36	4.69
Dense Veg.	8.27	415.66	51.35	2.66	477.94
Sparse Veg.	2.07	67.91	25.32	0.25	95.55
Water	0.4	5.01	0.43	0.91	6.75
Total	13.35	489.61	77.79	4.18	
		2001-2010	km^2		
Built Up	3.62	6.65	1.33	1.8	13.4
Dense Veg.	11.78	366.92	97.47	13.47	489.64
Sparse Veg.	4.72	56.25	14.5	2.22	77.69
Water	0.71	1.88	0.24	1.35	4.18
Total	20.83	431.7	113.54	18.84	
		2010-2024	km^2		
Built Up	12.8	3.93	3.95	0.22	20.9
Dense Veg.	35.52	330.38	19.6	45.8	431.3
Sparse Veg.	11.72	69.06	30.13	2.9	113.81
Water	2.22	5.97	0.35	10.36	18.9
Total	62.26	409.34	54.03	59.28	

Table 14: Average changes in channel width of the upper section

Year	Section	Avg_Width	Std_Ddev	% Change	Sinousity
1991	Upper	56.34	14.07	-	1.615
2001	Upper	72.24	18.92	28.20	1.638
2010	Upper	114.12	44.24	102.60	1.646
2024	Upper	168.63	97.53	199.30	1.727

The sinuosity of this section initially began at 1.615 in 1991. Then it increased slightly to 1.638 by 2001, continued its upward trend to 1.646 in 2010, and further increased to 1.727 by 2024, indicating a progressive tendency towards a more tortuous or meandering channel planform in the upper reaches of the river over the study duration. It suggests that the river is developing more pronounced bends and curves in response to factors such as changes in sediment type, alterations in flow regime that favour meander development, or the river extending its length to dissipate energy over a longer course. Figure 12 visually confirms this gentle, but continuous upward slope across the four time points, illustrating the ongoing increase in the river's meandering character.

Discussion

The findings on LULCC patterns and driving factors in the Ankobra River basin underscore the dynamic evolution inherent in natural systems such as that of rivers. River systems are fundamentally active and constantly changing. The significant and consistent increase in built-up areas over the different periods in the various sections of the river, coupled with a decrease in dense and sparse vegetation observed over much of the study period in the different parts of the river's section, clearly reflects profound human impact on the landscape. Even though river channel changes, such as bank erosion and accretion, are naturally occurring processes. Thus, they also reflect the aperiodic, non-repeating nature spatio-temporal dynamism of chaotic systems, where the system is constrained within certain limits but never follows the same path twice (Stecca & Hicks, 2022).

However, the observed spatial-temporal dynamism of the Ankobra River (Figures 12–14) provides empirical evidence of non-linear divergent evolution, as the Ankobra River reaches are following radically different trajectories despite similar forcing which occurs when two initially similar states become increasingly different over time due to internal feedback, a hallmark of chaotic systems (Phillips, 2006). Thus, in the upper section, the average channel width expanded by nearly 200% (from 56.34m to 168.63m), but the Standard Deviation exploded from 14.07m to 97.53m (Table 11). This massive increase in variance signifies that the river is not widening uniformly; rather, nearby reaches are following radically different trajectories despite facing similar anthropogenic forcing. Mathematically, this mirrors the exponential divergence of trajectories in a phase space, where small localized differences in bank resistance or sediment pulses are amplified into macroscopically heterogeneous patterns, therefore, the approximate present cannot be used to predict the long-term future, a phenomenon identified as the Butterfly Effect (Stecca & Hicks, 2022). Nonetheless, these diverging trajectories are often constrained by a strange attractor, meaning the river's configuration in terms of its width and sinuosity is always changing but remains bounded by the system's physical limits (Baas, 2002).

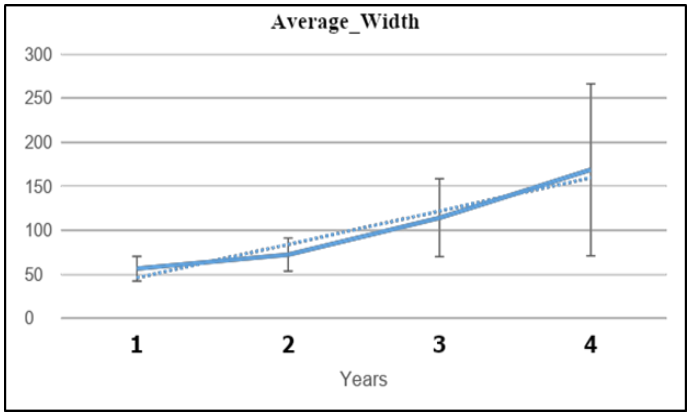

Figure 10: Average changes in channel width of the upper section

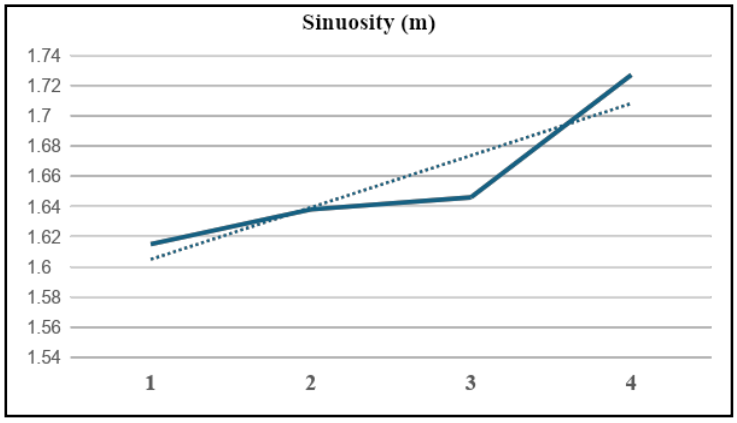

Figure 11: Average changes in sinuosity of the upper section

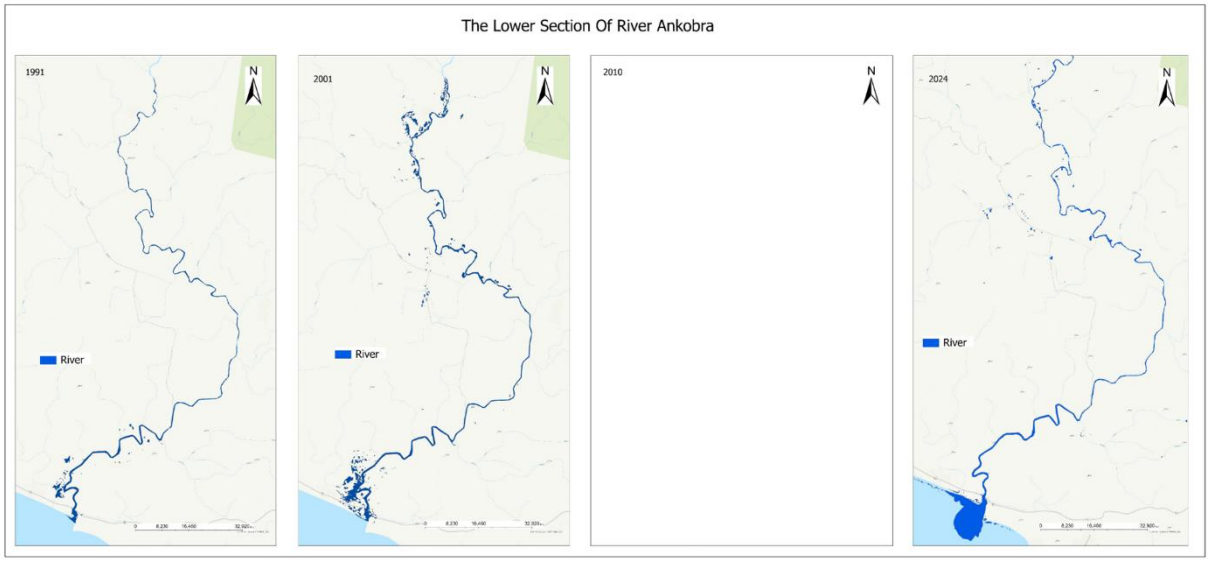

Figure 12: Lower section of River Ankobra from 1991-2024

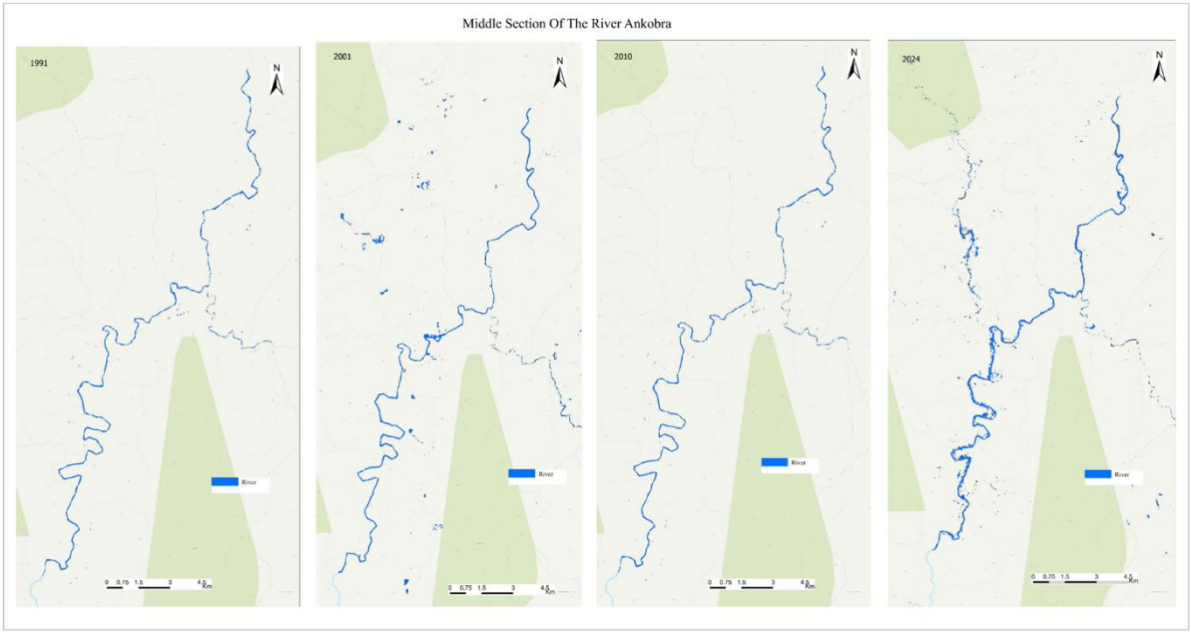

Figure 13: Middle section of River Ankobra from 1991-2024

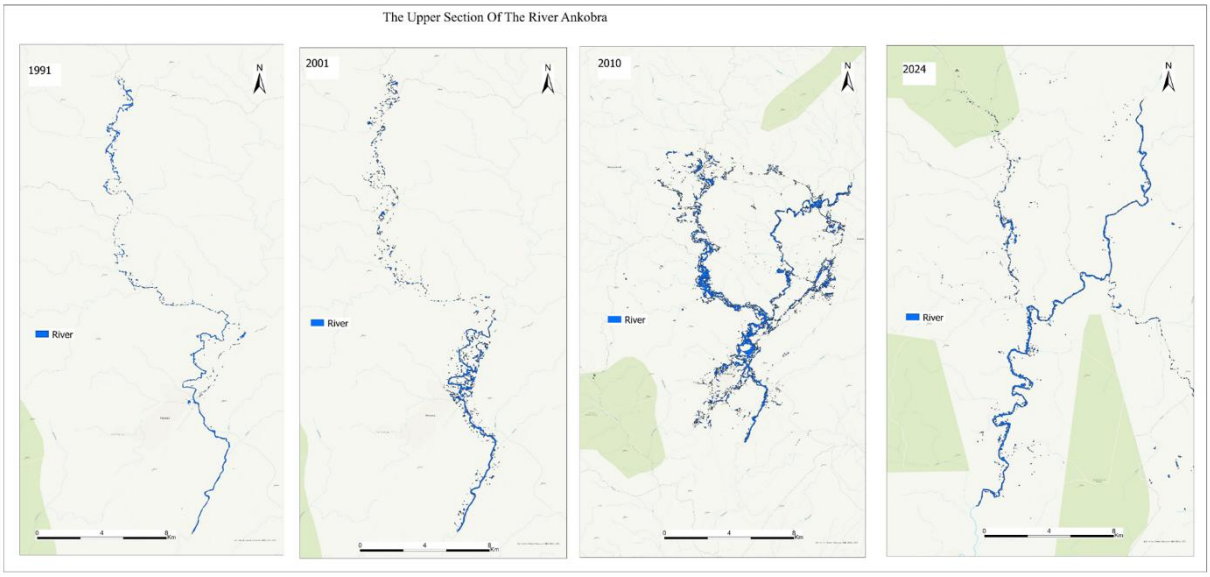

Figure 14: Upper section of River Ankobra from 1991-2024

The middle section (Table 9) exhibits a classic bifurcation. For two decades (1991–2010), the channel remained relatively stable with minor width changes (<2%). However, between 2010 and 2024, the system reached a threshold, resulting in a 61.50% expansion. This character of the middle section aligns with theoretical and empirical models of geomorphic bifurcation, geomorphic threshold, and deterministic chaos. In geomorphic systems, thresholds represent critical points where a system undergoes an abrupt change of state without necessarily experiencing a proportional change in external forcing (Gawler, 2002). The middle section after 2010 reached a critical value, where the system crossed a bifurcation point, moving from a predictable state into a high-energy, unstable regime (Zolezzi et al., 2012). A distinction can therefore, be made between the Stable/Periodic Attractor (1991–2010) where the system was in steady state while its development was constrained and followed a repeatable, predictable cycles and a Strange Attractor (2010–2024) where trajectories were bounded, but never repeat exactly (Okyere & Pacchi, n.d.).

The findings regarding the Ankobra River's morphology align closely with the tenets of the theoretical frameworks of Self-Organised Criticality (SOC) and Deterministic Chaos, where system responses are spatially and temporally contingent rather than linearly proportional to human "forcing". The observation that the upper section's sinuosity is consistently increasing toward higher values (1.727) places it on a trajectory toward geomorphic bifurcation. According to the SOC models, meandering rivers tend to evolve toward a critical sinuosity limit (theoretically $\pi \approx 3.14$ for unconstrained systems). While 1.727 is below the absolute theoretical maximum, the non-uniform widening observed suggests the river is entering a "supercritical" state relative to its local constraints where even a minor event can trigger a chain reactions or sudden reoganisation known as avulsion by which a chaotic system regains order, shifting the channel from an unstable high-sinuosity state to a more efficient, lower-sinuosity path (Hooke, 2023).

Conclusions and Recommendations

River systems are on a continual trajectory where their future behaviour is critically dependent upon what happens in the present, what went on in the past, and what is taking place in upstream and downstream reaches. A critical insight emerging from our findings is that these observed changes are not merely linear responses to singular drivers, but a manifestation of non-linear dynamics, and in many cases, deterministic chaos. This finding implies that

river systems exhibit a sensitive dependence on initial conditions, meaning that even minute, imperceptible differences in starting conditions can lead to macroscopically different and unpredictable long-term channel configurations. Additionally, since the effects of human activities and natural processes are spatially and temporally diverse, predictability is limited as is a one-size-fits-all management approach. Instead, the focus should be shifted to quantifying uncertainty and understanding the statistical behaviour and behavioural tendencies of the system. Moreover, by leveraging Advanced Earth Observation Technologies like Remote Sensing (RS) and GIS, quantification of river channel changes at unprecedented scales and resolutions is made possible. However, the exploratory nature of this study indicates the need for more in-depth research to understand the complexities of the Ankobra River's morphology. It is therefore, recommended that future research should focus on a multi-disciplinary approach, integrating hydrological data (such as rainfall, discharge, and eustatic factors), satellite imagery analysis, and ground-based surveys to create a more comprehensive model of the river's behaviour. This would provide a stronger evidence -based proposal for the development of sustainable river basin management strategies that would promote ecological resilience while promoting the wellbeing of communities that depend on the river for their livelihoods.

Declaration of interest

The authors declare no conflicts of interest

References

Affum, A. O., Kwaansa-Ansah, E. E., & Osae, S. D. (2024). Estimating groundwater geogenic arsenic contamination and the affected population of river basins underlain mostly with crystalline rocks in Ghana. *Environmental Challenges*, 15, 100898. https://doi.org/10.1016/j.envc.2024.100898

Amofa-Appiah, J. (2019). *Morphology of the Kakum River: a study on a small forested River in the Central Region, Ghana* (Doctoral dissertation, University of Cape Coast).

Asare, A., Asamoah, B. D., & Sanful, P. O. (2019). Assessment of Heavy Metal Contaminants Using Pollution Indices in Ankobra River at Prestea Huni-Valley District, Ghana. *Journal of Geoscience and Environment Protection, 07*(09), 25–35. https://doi.org/10.4236/gep.2019.79003

Awuah, G. K. (2016). Assessment of heavy metal concentrations in sediment, water and fish from the Ankobra and Tano river basins in Ghana. Masters Thesis, University of Ghana. http://ugspace.ug.edu.gh

Baas, A. C. (2002). Chaos, fractals and self-organization in coastal geomorphology: simulating dune landscapes in vegetated environments. *Geomorphology, 48*(1-3), 309-328.

Baynes, E. R. C., Lague, D., Steer, P., Bonnet, S., & Illien, L. (2020). Sediment flux-driven channel geometry adjustment of bedrock and mixed gravel–bedrock rivers. *Earth Surface Processes and Landforms*, *45*(14), 3714–3731. https://doi.org/10.1002/esp.4996

Boothroyd, R. J., Williams, R. D., Hoey, T. B., Brierley, G. J., Tolentino, P. L. M., Guardian, E. L., Reyes, J. C. M. O., Sabillo, C. J., Quick, L., Perez, J. E. G., & David, C. P. C. (2025). Big data show idiosyncratic patterns and rates of geomorphic river mobility. *Nature Communications, 16*(1), 3263. https://doi.org/10.1038/s41467-025-58427-9

Candel, J. H. J., Makaske, B., Kijm, N., Kleinhans, M. G., Storms, J. E. A., & Wallinga, J. (2020). Self-constraining of low-energy rivers explains low channel mobility and tortuous planforms. *The Depositional Record*, *6*(3), 648–669. https://doi.org/10.1002/dep2.112

Church, M., & Ferguson, R. I. (2015). Morphodynamics: Rivers beyond steady state. *Water Resources Research, 51*(4), 1883–1897. https://doi.org/10.1002/2014WR016862

Cunico, I., Bertoldi, W., Caponi, F., Dijkstra, H. A., & Siviglia, A. (2024). River ecomorphodynamic models exhibit features of nonlinear dynamics and chaos. *Geophysical Research Letters, 51*(11), e2023GL107951.Preprints. https://doi.org/10.22541/essoar.170431123.36024715/v1

Dong, T. Y., & Goudge, T. A. (2022). Quantitative relationships between river and channel-belt planform patterns. *Geology*, *50*(9), 1053–1057. https://doi.org/10.1130/g49935.

Durante, L., Tambroni, N., & Pittaluga, M. B. (2025). Multiple equilibrium configurations in river-dominated deltas. *Earth Surface Dynamics, 13*(3), 455-471. https://doi.org/10.5194/esurf-13-455-2025

Frascati, A., & Lanzoni, S. (2010). Long-term river meandering as a part of chaotic dynamics? A contribution from mathematical modelling. *Earth Surface Processes and Landforms*, *35*(7), 791–802. https://doi.org/10.1002/esp.1974

Gawler, M. (2002). Strategies for wise use of wetlands: Best practices in participatory management : proceedings of a Workshop held at the 2nd International Conference on Wetlands and Development (November 1998, Dakar, Senegal). Wetlands International ; IUCN, The World Conservation Union : WWF, World Wide Fund for Nature.

Giri, F., & Devercelli, M. (2023). Chaos arising from the hydrological behaviour of a floodplain river during the last century. *River Research and Applications, 39*(2), 241–254. https://doi.org/10.1002/rra.4080

Hasan, M. F., Shefa, M. S., Hasan, M. J., Islam, R., Kamal, K. M., Rukshana, F., Akter, A., & Shamsuzzoha, M. (2025). Linking River Morphodynamics and Land Use Land Cover (LULC) Changes: An Assessment of Riverbank Dynamics of the Bishkhali River.

Hooke, J. (2023). Morphodynamics of active meandering rivers reviewed in a hierarchy of spatial and temporal scales. *Geomorphology, 439*, 108825. https://doi.org/10.1016/j.geomorph.2023.108825

Kim, I., Jeong, G., Park, S., & Tenhunen, J. (2011). Predicted land use change in the Soyang river basin, South Korea. In *2011 TERRECO Science Conference, Karlsruhe Institute of Technology, Garmisch-Partenkirchen, Germany* (pp. 2-7).

Kyuka, T., Okabe, K., Shimizu, Y., Yamaguchi, S., Hasegawa, K., & Shinjo, K. (2020). Dominating factors influencing rapid meander shift and levee breaches caused by a record-breaking flood in the Otofuke River, Japan. *Journal of Hydro-Environment Research*, *31*, 76–89. https://doi.org/10.1016/j.jher.2020.05.003

Lane, S. N., & Richards, K. S. (1997). Linking River Channel Form and Process: Time, Space and Causality Revisited. *Earth Surface Processes and Landforms, 22*(3), 249–260. https://doi.org/10.1002/(SICI)1096-9837(199703)22:

Langat, P. K., Kumar, L., & Koech, R. (2019). Monitoring river channel dynamics using remote sensing and GIS techniques. *Geomorphology, 325,* 92–102. https://doi.org/10.1016/j.geomorph.2018.10.007

Okyere, S. A., & Pacchi, C. (n.d.). Mining, Environment and Community Conflicts: A study of Company- Community conflicts over gold mining and its implications for local community planning in Ghana.

Osman, A., Nyarko, B. K., & Mariwah, S. (2016). Vulnerability and risk levels of communities within Ankobra estuary of Ghana. *International Journal of Disaster Risk Reduction, 19*, 133–144. https://doi.org/10.1016/j.ijdrr.2016.08.016

Petrovszki, J., Timár, G., & Molnár, G. (2014). Is sinuosity a function of slope and bankfull discharge? – A case study of the meandering rivers in the Pannonian Basin. *Copernicus GmbH*. https://doi.org/10.5194/hessd-11-12271-2014

Pattison, I., & Lane, S. N. (2012). The link between land-use management and fluvial flood risk: A chaotic conception? *Progress in Physical Geography: Earth and Environment, 36(1),* 72–92. https://doi.org/10.1177/0309133311425398

Phillips, J. D. (2006). Deterministic chaos and historical geomorphology: A review and look forward. Geomorphology, 76(1–2), 109–121. https://doi.org/10.1016/j.geomorph.2005.10.004

Rego-Costa, A., Débarre, F., & Chevin, L.-M. (2017). Chaos and the (un)predictability of evolution in a changing environment. *Evolution*, *72*(2), 375-385. https://doi.org/10.1101/222471

Ruiz-Villanueva, V., Piégay, H., Scorpio, V., Bachmann, A., Brousse, G., Cavalli, M., Comiti, F., Crema, S., Fernández, E., Furdada, G., Hajdukiewicz, H., Hunzinger, L., Lucía, A., Marchi, L., Moraru, A., Piton, G., Rickenmann, D., Righini, M., Surian, N., … Wyżga, B. (2023). River widening in mountain and foothill areas during floods: Insights from a meta-analysis of 51 European Rivers. *Science of The Total Environment*, *903*, 166103. https://doi.org/10.1016/j.scitotenv.2023.166103

Scherelis, V., Doering, M., & Laube, P. (2023). HydroWidth: A small-scale approach to calculate river width and its variability. *Transactions in GIS, 27*(5), 1503–1525. https://doi.org/10.1111/tgis.13083

Shen, B.-W. (2025). *Lorenz's Models (1960–2008): Insights into Predictability Science*. https://doi.org/10.13140/RG.2.2.17125.72164

Singh, S. K., Laari, P. B., Mustak, Sk., Srivastava, P. K., & Szabó, S. (2018). Modelling of land use land cover change using earth observation data-sets of Tons River Basin, Madhya Pradesh, India. *Geocarto*

International, 33(11), 1202–1222. https://doi.org/10.1080/10106049.2017.1343390

Stecca, G., & Hicks, D. M. (2022). Numerical Simulations of Confined Braided River Morphodynamics: Display of Deterministic Chaos and Characterization Through Turbulence Theory. *Journal of Geophysical Research: Earth Surface, 127*(3), e2021JF006409. https://doi.org/10.1029/2021JF006409

Sukarno, R. H. T. H., Intansari, F., Shidiq, I. P. A., Hernina, R., & Kusratmoko, E. (2019). The Effect of Jatigede Dam Construction towards the Spatial Pattern of Total Suspended Solids and Chl-a in Waters Areas around Mouth of Cimanuk River. *IOP Conference Series: Earth and Environmental Science*, *338*(1), 012020. https://doi.org/10.1088/1755-1315/338/1/012020

Whitbread, K., Jansen, J., Bishop, P., & Attal, M. (2015). Substrate, sediment, and slope controls on bedrock channel geometry in postglacial streams. *Journal of Geophysical Research: Earth Surface*, *120*(5), 779–798. https://doi.org/10.1002/2014jf003295

Yin, R. K. (2016). Qualitative Research: from start to finish (2nd Ed). The Guildford Press, UK.

Zhang, Y. (2024). *Interplay of Discharge Rates, Slope, And Sediment Size in River Meandering Dynamics: Insights From Experimental Studies* [Master of Science in Environmental Engineering, Michigan Technological University]. https://doi.org/10.37099/mtu.dc.etdr/1870

Zolezzi, G., Luchi, R., & Tubino, M. (2012). Modeling morphodynamic processes in meandering rivers with spatial width variations. *Reviews of Geophysics, 50*(4), 2012RG000392. https://doi.org/10.1029/2012RG000392